Chapter 7
Flood Risk Management Modelling in the River Ibar Catchment Area

Srđan Jović and Jelena Đokić

Abstract In this paper, there are presented the risk assessment modeling of all rivers in the River Ibar Catchment that have been flooding or have a potential for flooding of agriculture land, houses, roads, bridges, and other objects. For each river, those flooded or potentially flooded surfaces are presented by category of risk (high risk, medium risk, and low risk) as well as the causes of the flooding and recommendations for short term and long term activity protection against floods. All inputs for the flood risk assessment (water cycle analysis, lake-level prediction, evapotranspiration, climatic conditions) were simulated by using different modeling techniques. By analyzing the locations and vicinity of the human activities, it sets the river priority for intervention. This is enabled by the information presented through the Geographical Information System Elements (GIS) of the Water Framework Directive. Although the information presented by GIS depends on the availability of the spatial and field data, it is a valuable tool in risk assessment in determining the cumulative sensitivity of the specific region to the floods.

Keywords Floods · Evapotranspiration · Evolutionary algorithm · Sensorless estimation · Neuro-fuzzy approach · GIS

7.1 Introduction

Floods take place almost every year in North of Kosovo*. Recently, the floods have happened in approximately the same locations in 2013, 2014 and 2015. Luckily, there were no human victims, but there were significant damages on infrastructures, agriculture and roads. It was evaluated that any consequences of floods could have been avoided if basic principles of safe behaviour had not been ignored. Recommendations on flood prevention mainly include necessary measures that should be taken to physically prevent the devastating impact of floods. Necessary preventive measures should also be taken at the legislative level and in legislation enforcement.

S. Jović · J. Đokić (✉)

Faculty of Technical Sciences, University of Pristina, Kosovska Mitrovica, Kosovo
e-mail: jelena.djokic@pr.ac.rs

The climate change has made profound changes in water cycles and produced serious water problems and water crisis in many areas. The main reason is that the structure and the parameters of the water cycle have evolved under the influence of human activities and consequently resulted in the reduction of runoff water resources. In order to understand the changes in the water cycle in the changing climatic conditions, the scientists should analyze the overall water cycles. Human cycle of water was investigated by identifying potential exposure pathways for water contamination, as well as understanding the potential impact of contaminated water in the case of floods. This study area is in the specific situation having some five mining waste deposits situated along the river Ibar, which contain toxic and hazardous substances from the lead and zinc ore processing (Milentijevic et al. 2013).

In the more detailed analysis, the enhanced activity of the water cycle as important part for protecting the photosynthetic apparatus was investigated (Weng et al. 2008). The relation between natural and social aspects of the water cycle was analyzed and some four aspects of dualistic water cycle evolution were discussed in Qin et al. (2014). Water storage is significant for understanding water cycles of global and local domains and for monitoring climate and environmental changes (Xu et al. 2013). Actual evapotranspiration is a vital process of the water cycle that links land surface water balance and land surface energy balance (Itier et al. 1992; Gerla 1992). Evapotranspiration plays a key role in simulating the hydrological effect of climate change (Xu et al. 2016; Blum and Gerig 2006). In Zhao et al. (2013), the evapotranspiration estimation methods applied in hydrological models were summarized. The dominant role of transpiration in comparison with other components of evapotranspiration was illustrated in vegetation in the annual cycle (Buchtele and Tesar 2009). Decreasing trends in annual precipitation and potential evapotranspiration could lead to a decrease in actual evapotranspiration in the basin (Gao et al. 2012). The importance of estimation of actual evapotranspiration was recognized a long time ago (Rana et al. 1997), and the estimation model is tested on the field. How evapotranspiration and water availability had changed in the changing climatic conditions in Northern Euroasia has been evaluated in (Liu et al. 2014). In the water science, the estimation of evapotranspiration is extensively investigated topic (Dong et al. 2016). A long term precipitation analysis and estimation of precipitation concentration were done by using support vector machine method (Gocic et al. 2016). In order to reduce water losses, the evapotranspiration, evaporation, and seepage losses in arid and semi-arid region were investigated (de la Paix Mupenzi et al. 2012). The emphasize was also put on the better analysis of the water cycle and monthly average evapotranspiration in the area (Morari and Giardini 2001). Estimating the evapotranspiration is based on different climatic parameters such as air temperature, vapor pressure, and humidity. The reliability of the estimation of the reference evapotranspiration by simplified pan-based approach, that do not require data on relative humidity and wind speed, was analyzed by comparing the estimated results with the lysimeter measurements on the field (Trajkovic et al. 2010). The monitoring process generates a large number of data. The application of artificial neural networks in the forecasting the reference evapotranspiration has been used for a long time now

(Kisi and Yildirim 2005). Neuro-fuzzy approach (Jang et al. 1997) was used for the process of modelling, as evapotranspiration has a strong fluctuations during the year.

Lake-level prediction is very important for sustainable management of local and regional water resources (Tongal and Berndtsson 2014; Shafaei and Kisi 2016). However, reliable prediction of groundwater level is also essential for water resource management (Gong et al. 2016). Modeling lake-level fluctuation is essential for planning and designing of hydraulic structures along the lake coasts (Sanikhani et al. 2015). This issue becomes important, as traditional lake-level fluctuations is changed due to the climate change (Kakahaji et al. 2013). Prediction of water-level fluctuations in lakes is a necessary task in hydrological and limnological studies (Vaheddoost et al. 2016).

Soft computing methods became very useful tool for solving different engineering problems (Verplancke et al. 2008; Meng and Xia 2007; Cai et al. 2010). One of the most often used soft computing methods is Support Vector Regression (SVR) approach. However, the SVR approach is highly dependent on the proper selection of the parameters. There were many strategies proposed for the parameter selection, but most of the strategies are restricted for linear cases or prone to local minima. Soft computing approach was also used for sensorless estimation of the lake level (Jovic et al. 2018b).

A watercourse of the river Ibar downstream of the artificial lake Gazivode is largely impacted by the lake. The lake Gazivode was constructed in the 1970s. Its purpose was to regulate the river Ibar flow, produce electricity and irrigate Kosovo plain for agriculture production. The final result of the study should be a detailed analysis of the flood risk in the research area.

7.2 Methods and Materials

7.2.1 Study Area

This section presents the respective information regarding the existing environmental and social baseline conditions of North Kosovo and summarizes the information currently available, which may potentially be affected by the floods in the four municipalities Leposavic, Zubin Potok, Zvečan and Kosovska Mitrovica.

The detailed baseline characterization will be used as input to identify possible project impacts and assess their acceptability in terms of environmental and social effects. This part is based on existing data and information and includes a description of the environmental and socioeconomic conditions baseline.

7.2.2   Physical Environment

Project is affecting four municipalities, which are located in the north part of Kosovo. This particular part of Kosovo is specific for its geographic, social and environmental features.

Kosovo varies in elevation from 265 to 2656 m above mean sea level (amsl), with approximately 77% of its area lying between 500 and 1500 m amsl. Higher altitude areas, above 1500 m, cover approximately 6% of the area and are significant from a biodiversity standpoint. Kosovo is very diverse geologically, with volcanic, metamorphic, and sedimentary rocks of varying ages and origins present. The soils are generally nutrient-rich, providing a good growth medium for natural plants and crops. Limestone is located in several parts of Kosovo and has weathered to form a distinctive topography that includes numerous caves. Soils derived from limestone and ultra-basic serpentine rocks have chemical characteristics that restrict plant growth to specially adapted species that are often restricted to these soil types. Many stretches of rivers have been severely disrupted by sand and gravel mining and attempts to control river flooding with artificial levees.

The study concerns four municipalities, which are located in the north part of Kosovo*. This particular part is specific for its geographic, social, and environmental features. This region is geographically located in 420 53″ N and 200 53″ E, and it has altitude between 508 and 510 m. It has around 154 km². Dominant forms of relief are volcanic cone in the form of Zvecan hill (797 m in height) and firth of river Sitnica into river Ibar. From the east, north, and west, the region is surrounded by mountains Kopaonik, Rogozna and Mokra Gora. Through the region, three main rivers are flowing: Ibar, Sitnica, and Ljusta. This represents a very good geographical position for all human activities, industry, and agriculture (Fig. 7.1).

7.2.3   Climatic Conditions

The morphological, i.e., hypsometric characteristics of the terrain have impacted Northern Kosovo climate characteristics. The Climate is temperate-continental to mountain climate. The mountain ranges of Mokra Gora, Rogozna, Suva Planina and southern and south-western slopes of Kopaonik have their specific impacts in climate characteristics. For the analysis of the parameters, the data of precipitations, temperatures, sunshine, wind, and humidity are obtained from the climatology stations Kopaonik, Novi Pazar, Mitrovica, and Pec, surrounding the terrain. These parameters are used for the analyzed period from 1961 to 1999. From 1999 until 2014, the data were obtained from the meteorological stations presented in Table 7.1.
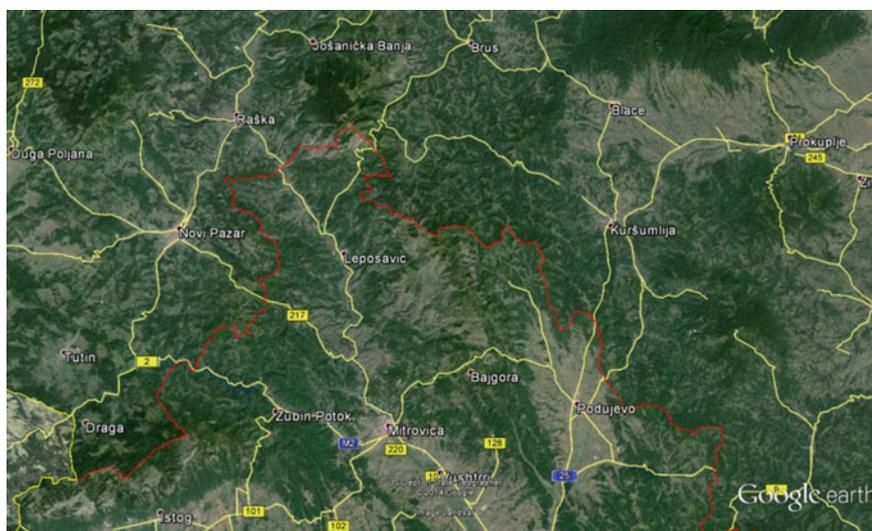
Fig. 7.1 Location map of study area according to the topographical map (Google Earth 2019)

Also, for the precipitation analysis the data from Climatic Atlas are used. In that time the precipitation stations were numerous in this region (Ribarići, Brnjak, Režala, Kosovska Mitrovica, Banjska, Vlahinje, Leposavic and Lesak).

Air Temperature
The influence of the mountain range is obvious in the analysis of the temperature regime. The air temperature in the highest parts is reaching $-30\,°C$, during the winters. So, the average temperature in the research area varies from 3.7 (CS Kopaonik) to 11.4 °C (CS Peć). The coldest month is January, with mean temperature from $-4\,°C$ CKS Kopaonik) to 10 °C (CS Peć). August is the hottest with mean temperature varying from 13 °C (CS Kopaonik) to 22.1 °C (CS Peć).

The altitude, micro-climate, and spatial distribution of the relevant climate stations reflect the conditions on the site, so the data are valid for this research terrain. As shown in the Fig. 7.2 the minimum and maximum daily temperatures keep the correlation throughout the year, what is significant for the water level estimation.

Precipitation and Humidity
Based on the available data, it can be seen that there are relatively small oscillations of precipitations during the year, or that the precipitations are evenly distributed throughout the year. That is very good from the hydrology point of view, as that stable regime enables stabile regime of the ground waters. The average precipitations for the region are 600–855 mm on the mountain slopes Kopaonik, Mokra gora, and Suva planina, in strong winters the number of days with snow is up to 180, effecting significantly the ground waters. Most of the precipitations are recorded in April, May, and October. Based on the collected data for the minimum relative humidity in

Table 7.1 Meteorological stations surrounding research terrain

|	Longitude (°)	Latitude (°)	Altitude (m)	Distance (km)	Direction	Direction	Station Name	Country Name
1	20.7	43.7	217	91.1	351	N	Kraljevo	Serbia
2	21.9	43.33	202	96.9	59	NE	Nis	Serbia
3	21.65	41.96	239	121.6	148	SE	Skopje-petrovac	North Macedonia
4	22.28	42.51	1176	122.7	110	E	Skopje	North Macedonia
5	19.28	42.43	52	139.7	249	W	Podgorica	Montenegro
6	19.25	42.36	33	145.1	247	SW	Podgorica-Golubovci	Montenegro
7	20.7	41.53	1321	151.9	185	S	Lazaropole	North Macedonia
8	22.18	41.75	327	166.3	139	SE	Stip	North Macedonia
9	23.38	42.65	595	206.6	97	E	Sofia-(observ.)	Bulgaria
10	21.36	41.05	589	208.6	169	S	Bitola	North Macedonia
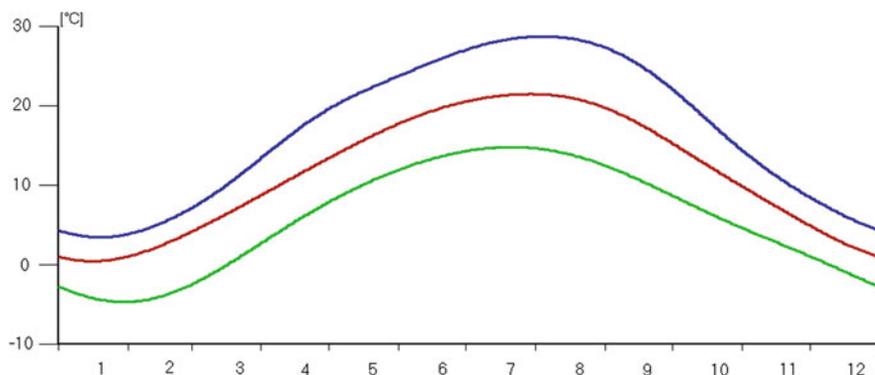
Fig. 7.2 Graphic presentation of the temperature regime in North Kosovo, minimum (green), maximum (blue) and mean (red) (Color figure online)

Table 7.2 Statistic data for daily precipitation and evapotranspiration in Northern Kosovo Region

Day	Prec.	Prec.	Prec.	PET	PET	PET
	Best (mm)	Low (mm)	High (mm)	Best (mm)	Low (mm)	High (mm)
Mean	8.35	5.54	13.48	1.92	1.63	2.21
Min.	10.00	0.00	2.25	0.35	0.01	0.66
Max.	42.40	31.95	66.56	3.99	3.59	4.48

the region of interest in the last 20 years (Djokic et al. 2012), it can be concluded that the periods of heavy rains in April and May are followed by extreme dry weather in late July and August.

The results from Table 7.2 are presented in the graphic presentation in the Fig. 7.3 while Kosovo's precipitation map is presented in Fig. 7.4.

Solar Radiation

Kosovo has, on average 2066 h with sun per year or approximately 5.7 h per day. The highest insolation value is in Pristina with 2140 h for one year, while Peć with the smallest insolation value of 1958 h, Uroševac with 2067 h and Prizren with 2099 h. The maximum insolation in Kosovo occurs during July, while the lowest insolation occurs in December.

Distribution of general solar radiation for Northern Kosovo is given in Table 7.3. Throughout the year the sunshine hours are presented in Fig. 7.5.

Wind

Considering the terrain properties in the North Kosovo*, and the study area of the river Ibar valley, the winds are relatively slow, and do not have influence on the occurrence of floods. The annual wind velocity statistics is presented in the Table 7.4.

Data collected on daily basis are presented in the graphic presentation in Fig. 7.6. As shown in the figure, the most of the winds are concentrated in July–August, in
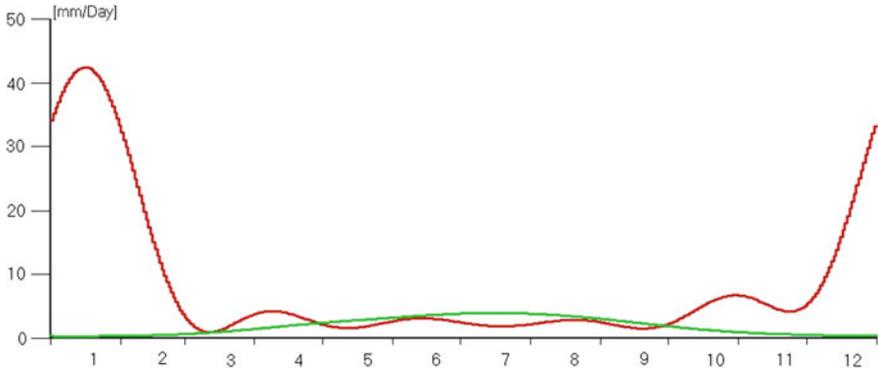
Fig. 7.3 Average daily precipitation (red) and evapotranspiration (green) in the North Kosovo (Color figure online)
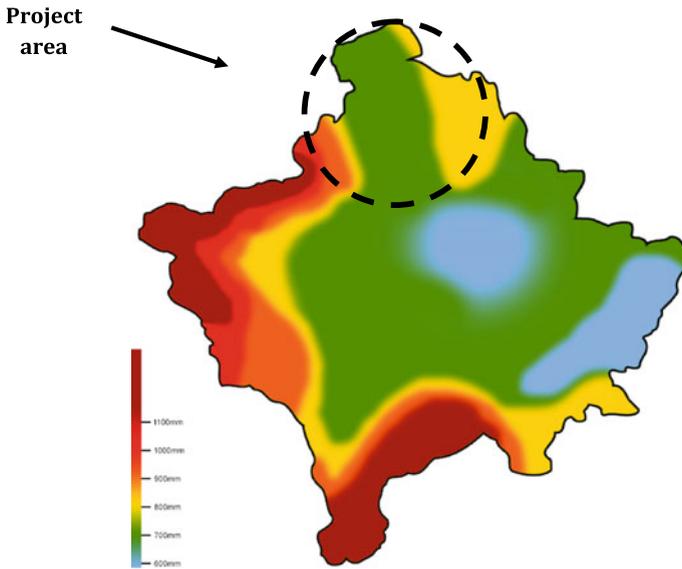

Fig. 7.4 Precipitation distribution of Kosovo

Table 7.3 Sunshine fractions and Sunny hours in North Kosovo* region

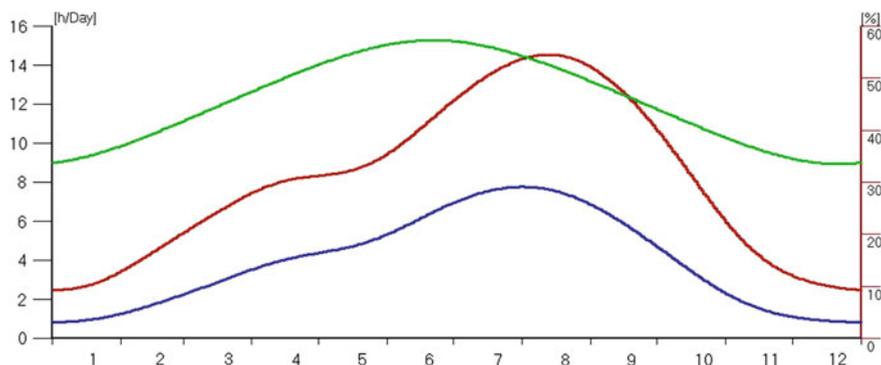| Day	Sun Fr.	Sun Fr.	Sun Fr.	Sun Hrs.	Sun Hrs.	Sun Hrs.	Day Len.
	Best (%)	Low (%)	High (%)	Best (h)	Low (h)	High (h)	(h)
Mean	30.333	22.273	38.923	3:57	3:01	4:55	2:09
Min.	9.35	0	21.74	0:50	0:00	1:57	8:56
Max.	54.5	50.05	60.9	7:45	7:07	8:30	5:15

Fig. 7.5 Annual sunshine cycle in Northern Kosovo Red: Sunshine fraction [%], Green: Daylength [h], Blue: Sunshine hours

Table 7.4 Wind velocity distribution in km/h throughout the year in North Kosovo*

Day	Vapor Best (hPa)	Vapor Low (hPa)	Vapor High (hPa)	Wind Best (km/h)	Wind Low (km/h)	Wind High (km/h)
Mean	10.617	9.068	12.165	3.42	1.01	6.14
Min.	4.98	4.01	5.84	2.25	0	4.53
Max.	16.9	14.82	19.09	5.55	3.52	7.92

the north-south direction, bringing hot weather from the south along the river Vardar valley, and contributing the river pollution from the surrounding industrial toxic waste deposits by fumigation (Milentijevic et al. 2013).
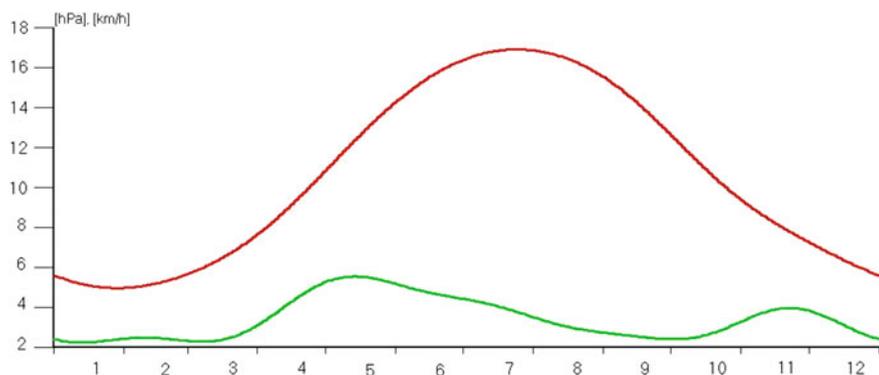

Fig. 7.6 Wind velocity in Zvecan municipality (red) and water vapour pressure (green) (Color figure online)

7.2.4 Hydrographic Data

The region of the North of Kosovo is in the region of Ibar Catchment Fig. 7.7. The spring of Ibar is on the territory of South-Eastern Crna Gora (Montenegro). In the area from Ribarice to Gazivode the river forms accumulation lake, whose waters are used for irrigation through the system Ibar—Lepenac, for water supply in Mitrovica region and electricity production. The Ibar catchment belongs to Black sea catchment, and it occupies the surface of 3593 km² that is one-third of Kosovo.

The direct catchment of Ibar includes the streams of the northern part of Mokra gora and Suva mountain, southern and south-eastern slopes of Rogozna and the region of southern and south-western Kopaonik on the right bank of Ibar, on the north side of the line Mitrovica—Stari Trg (peak Oštro Koplje, 1789 m), to the ore bodies Šatorica, Jelakce and Belo Brdo. The total surface of the direct Ibar catchment in Kosovo is 754 km². The catchment area is characterized by mountain relief with deeply cut Ibar valley and its tributaries. The largest altitude difference is 1339 m in Kopaonik region and in Suva planina area where the difference is 1283 m. Along the flow through Kosovo in 50 km, Ibar river is flowing downhill with an altitude difference of 209 m (659–450 m).
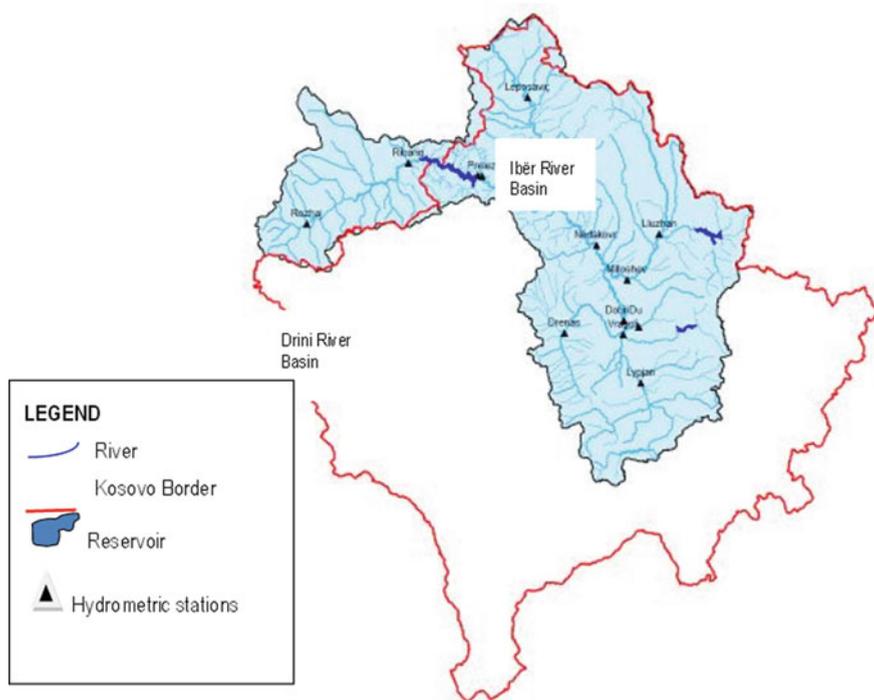

Fig. 7.7 The Ibar River Basin in Kosovo*. *Source* World Bank Document: Water Security for Central Kosovo No. 71850, 2011

On the west from Mitrovica, the Ibar catchment is developed in credo flysch, and on the northern slopes of Suva Mountain in Palaeozoic schist. On the north of Mitrovica, in the catchment, there is a predominant area of serpentines and peridotites (ultra basic massive) with penetration of eruptive rocks (dacite and andezite) as well as the minor zone of diabase-horn formations near the village Slatina. There is also some participation of Pliocene and Quarterly terraces, 5 km upstream from Mitrovica, near villages Žabare and Vinarce. The alluvial deposit has some small occurrence, in the plane as well as in profile. In the area of Vinarce, the depth of alluvium is just 5 m, and under this layer, there is credo flysh. In the village of Pridvorica the water nonpermeable clay layer occurs after just 4.5 m of alluvial deposit. Significant tributaries of the Ibar river are: Brnjačka, Čečevska, Sitnica, Banjska, Bistrica, Vučanska, Sočanska (in upper stream Mošnička, where there are no living organisms), Leposavska (collecting all mining waters from the mines Žuta Prla, Koporić and Jelakce), Jošanička, Drenska (cathing mining waters from the pit Belo Brdo) and Srpska Bistrica.

The hydrology properties of the region are analyzed, with data of flow in three water measuring profiles at the Ibar river (profiles: Batrage, Perlez, and Leposavić), for the observing period from 1991 to 2000. The characteristic flows are given in Tables 7.5 and 7.6.

7.2.5 HEC-RAS Hydrology Calculations

The HEC-RAS is numerical software for hydrology calculations (Kalaba et al. 2014). It is widely used in one-dimensional water surface profile calculations in case of steady and unsteady river flow regimes. Also, it contains components for one-dimensional sediment transport/movable boundary and river water quality numerical calculations (Kalaba et al. 2014).

As previously mentioned, the aim of this study was the preliminary analysis of the terrain and creation of the model for the further water quality and water flow analysis of the river Ibar flooding capacity between the artificial lake Gazivode and the city of Leposavic. The only major tributary of the Ibar in this area is the river Sitnica, and it flows into the Ibar beyond the observed section. In the studied sections, the river Ibar flows the series of dams which starts with the Gazivode, located at the end of the 24 km long artificial lake Gazivode, and the Pridvorica located around 2.3 km below the Gazivode. There is only one bridge, located between the Pridvorica and the village Zubin Potok, and it was not taken into mainly through the alluvial plain which is shortly interrupted after the village Varage, and nearby dam Trepča, in the length of approximately 2 km. The dam Trepca is the third in account in this analysis. The path of river reach is taken from topographic map loaded into the HEC-RAS geometric data editor. The reach starts few meters downstream of the dam Pridvorica, at the elevation of 578 m, and ends few meters upstream of the dam Trepca, at the elevation 553 m. Since the reach length is 6.67 km, sixty-eight initial cross-sections, labeled 0–67, were positioned at every 100 m. The distances between cross-sections

Table 7.5 Flow characteristics for Prelez for the observing period from 1991 to 1999

Catchment: Z. Morave	River: Ibar	Profile: Prelez	Waters observation method: linnigraf					Start: 1934	Elevation: 542.6		Km from the confluence: 182	Surface km²: 1109	
Months													
Year	Q (m³/s)	I	II	III	IV	V	VI	VII	VIII	IX	X	XI	XII
1991	NQ	1.32	1.56	1.32	1.32	3.14	1.56	1.68	4.82	4.38	7.32	8.4	3.94
	SQ	2.26	3.48	1.78	6.21	7.16	6.75	5.31	6.09	8.83	13.1	11.3	5.65
	VQ	65.1	49.5	30.6	83.4	68.1	68.1	99.3	53.6	84.6	80	70.2	69.1
1992	NQ	2.4	1.7	1.4	2.0	2.0	1.4	1.4	1.4	3.0	2.4	2.0	2.0
	SQ	13	2.54	2.68	2.86	2.43	1.99	2.44	2.52	5.91	3.95	4.07	2.52
	VQ	70.1	3.6	3.2	4	3.2	2.4	6.6	3.2	63.7	42.4	14.2	3.2
1993	NQ	4.52	5.3	2.6	2.4	1.7	1.7	1.55	0.92	0.81	0.92	2.8	1.7
	SQ	15.3	29.2	10.8	5.18	2.71	2.32	2.65	3.12	1.47	1.7	7.26	6.83
	VQ	66.9	81.2	71.1	8.25	4	3.6	47.6	9.57	3.0	4.52	38.4	16.4
1994	NQ	1.7	2.0	1.03	1.03	0.92	0.81	0.81	1.03	0.64	0.92	9.57	1.4
	SQ	2.28	13	1.51	1.5	1.39	1.26	2.6	2.48	1.28	10.3	28.4	17.1
	VQ	3.0	112	50.2	2.0	2.2	15.1	41.6	38.4	27.1	35.2	80	78.9
1995	NQ	1.4	1.14	1.03	1.7	1.55	2.6	2.4	1.55	1.4	1.03	0.92	1.14
	SQ	1.83	1.67	1.46	3.74	4.59	3.73	6.94	2.36	2.5	4.74	5.06	13.3
	VQ	2.4	2.0	30.7	33.3	28.2	26.5	75.6	29.4	50.2	62.7	58.7	70.1
1996	NQ	1.15	1.81	1.39	3.46	2.56	0.99	0.83	1.39	0.99	0.99	1.94	2.2
	SQ	11.8	13.6	13.9	7.11	5.73	2.45	1.66	1.61	1.33	1.81	2.08	68.7
	VQ	61.6	62.7	26.5	78.9	78.9	54.9	5.3	1.94	1.55	2.2	2.2	95.6

(continued)

Table 7.5 (continued)

Catchment: Z. Morave	River: Ibar	Profile: Prelez	Waters observation method: limnigraf						Start: 1934	Elevation: 542.6	Km from the confluence: 182	Surface km²: 1109	
Months	I	II	III	IV	V	VI	VII	VIII	IX	X	XI	XII	
Year	Q (m³/s)												
1997 NQ	0.83	1.22	1.22	1.15	1.22	19.9	6.44	1.02	0.83	0.96	0.96	0.96	0.83
SQ	54.8	29.7	3.45	1.41	23.4	39	12.6	16.2	4.05	1.16	1.03	1.05	15.6
VQ	62	59.9	26.4	2.38	49.4	74	16.5	55.6	19.4	14.4	1.09	1.09	74
1998 NQ	1.02	1.02	1.02	1.02	0.74	0.74	0.74	0.74	0.74	0.79	0.74	18.9	0.74
SQ	1.19	1.11	1.07	1.06	0.84	0.8	0.84	0.80	0.78	0.91	2.78	19.9	2.7
VQ	1.36	1.22	1.22	1.15	0.96	0.96	0.96	0.96	0.83	1.02	9.28	20.9	20.9
1999 NQ	18	2.16	1.22	1.02	57.8	49,4	47.3	0.96	0.57	18	18	12	0.56
SQ	19.3	14.6	1.51	5.25	75.8	51.6	51.3	29.6	33	19.2	19.3	15.4	28.1
BQ	20.9	19.9	2.16	14.4	93.6	53.5	53.5	53.5	53.5	19.9	19.9	19.9	93.6

Table 7.6 Flow characteristics for Leposavić for the observing period from 1991 to 1999

Catchment: Z. Morave		River: Ibar	Profile: Leposavić	Waters observation method: limnigraf				Start: 1934	Elevation: 445.3		Km from the confluence: 131		Surface km²: 4701	
Months / Year	Q (m³/s)	I	II	III	IV	V	VI	VII	VIII	IX	X	XI	XII	
1991	NQ	9.34	10.01	18	17	24	15.2	–	7.24	7.88	9.72	12	12.8	–
	SQ	12.3	22.0	33	45.7	33.3	21.4	–	8.79	10.5	13.5	18.8	21.8	–
	VQ	33.7	119.0	74.3	126	102	70.6	–	15.2	34.3	45.7	60.7	55.4	–
1992	NQ	13.2	13.2	11.6	14.8	10.9	11.6	10.1	8.2	7.56	7.88	8.96	11.6	7.56
	SQ	22.6	17.7	15.1	53.4	13.8	13.7	13.3	9.61	9.67	9.34	18.3	18.1	17.8
	VQ	59.9	56.3	29.5	135	23	28.5	38.1	37.4	38.8	11.2	72.0	56.3	135
1993	NQ	11.2	12.0	13.2	16.5	12.0	9.72	7.24	6.6	6.28	7.56	8.96	11.2	6.28
	SQ	20.8	32.0	36	41.9	17.0	11.5	8.24	7.81	7.3	7.91	11.0	16.6	18.1
	VQ	58.0	61.6	125	91.0	40.4	50.5	15.6	25.9	14.8	8.2	15.6	64.2	125
1994	NQ	20.0	21.0	12.4	12.0	11.6	10.1	9.72	5.64	6.28	–	–	–	–
	SQ	21.0	32.7	14.8	17.5	16.2	10.9	12.3	7.13	7.09	–	–	–	–
	VQ	23.0	51.8	22.5	53.6	24.0	12.8	66.2	9.34	8.2	–	–	–	–
1995	NQ	6.28	14.4	12.4	18.0	16.8	11.2	8.58	8.96	11.2	10.5	16.0	21.5	6.28
	SQ	13.7	18.2	15.1	45.9	29.1	14.5	13.7	11.2	15.9	16.2	24.5	40.3	21.5
	VQ	36.0	30.0	22.5	152	38.8	17.6	40.9	28.0	51.8	41.6	55.4	91.6	152
1996	NQ	16.8	18.8	23.5	36.0	19.2	7.56	7.88	7.88	9.72	12.4	13.2	37.4	7.56
	SQ	27.6	56.8	40.7	74.2	29.3	12.4	9.48	9.28	16.4	15.4	45.5	75.1	34.2
	VQ	74.0	244	118	156	53.6	19.2	15.6	19.2	33.6	34.8	163.0	206	244

Table 7.6 (continued)

Catchment: Z. Morave	River: Ibar	Profile: Leposavić	Waters observation method: limnigraf					Start: 1934	Elevation: 445.3		Km from the confluence: 131		Surface km²: 4701	
Months	I	II	III	IV	V	VI	VII	VIII	IX	X	XI	XII	
Year	Q (m³/s)													
1997 NQ	50	20.5	18	44.4	26	16	17.6	11.2	8.96	10.5	11.6	13.6	8.96
SQ	88	34.2	37.7	91.5	43.5	27.4	20.3	21.9	13.4	13.7	13.8	26.9	36
VQ	226	56.3	81.9	177	83.6	41.6	27	33	21.5	23	23.5	76.6	226
1998 NQ	13.6	14.4	16	16	15.2	6.92	4.5	6.28	9.72	14.4	16.8	29	4.5
SQ	16.3	31	23.6	20.9	21.1	13.3	6.03	7.45	15.3	21.6	32.1	59.4	22.3
VQ	19.2	94.3	60.6	53.6	30	22	8.96	8.96	21.1	43	63.8	174	174
1999 NQ	33.6	40.2	–	–	–	–	–	–	–	–	–	–	–
SQ	76.5	102	–	–	–	–	–	–	–	–	–	–	–
BQ	225	320	–	–	–	–	–	–	–	–	–	–	–

were adjusted, first to reach proper length, and afterward to achieve an appropriate position of each cross-section. Before the interpolation to a maximum distance of 20 m, additional cross-sections were added to all positions where it was necessary due to a sudden change in flow geometry. The geometry of cross-sections used in calculations was based on the WebGIS data (Kalaba et al. 2014). The Ibar river flow was analyzed from the thermal capacity evaluation point of view (Kalaba et al. 2014). In this study, the data on the turbine discharge from the hydroelectric power plant Gazivode was 30 m^3 s^{-1} will be used for calculation. The measurements were performed with precision and water flow meter P-770-M with probe Mini Water 6050-1008. The average velocity between the turbine discharge at Gazivode and the village Suvi Do is 1.12 ms^{-1}.

7.2.6 Neuro-Fuzzy Modeling

The neuro-fuzzy network represents the combination of neural networks and fuzzy logic methodology. The fuzzy methodology is the main part of the neuro-fuzzy network. The network has five layers. Each of the layers has a specific task in the estimation process. The main advantage of the neuro-fuzzy network is fuzzification of the input data and application of membership functions as fuzzy functions. By this way, one can avoid errors in experimental data. The neuro-fuzzy network is training by a back-propagation learning algorithm. Three statistical indicators were used to measure the neuro-fuzzy estimation accuracy. These factors were the root mean square error (RMSE) and the coefficient of determination (R^2). These two factors could fully measure the prediction accuracy of the neuro-fuzzy network.

7.3 Results and Discussion

The Ibar River flows through eastern Montenegro, Serbia and Kosovo, with a total length of 276 km. The river begins in the Hajla Mountain, in Rožaje, eastern Montenegro then passes through Kosovo and flows into the West Morava River, Central Serbia, near Kraljevo and to the Black Sea drainage basin. Its drainage area is 8059 km^2, the average discharge at the mouth 60 m^3/s. The river is not navigable. In its middle course, the river passes through Gazivode reservoir and Zubin Potok municipality, reaching the city of Kosovska Mitrovica. There it makes a sharp, elbow turn to the north flowing through Zvečan and Leposavić municipalities, entering Serbia at the village of Donje Jarinje. At Gazivode, the river is dammed, creating the artificial lake (area 11.9 km^2, altitude 693 m, depth 105 m).

Right on its elbow turn, the Ibar receives its longest (right) tributary, Sitnica. After its elbow turn and receiving the Sitnica, the Ibar flows through rather a narrow riverbed under the western slope of the Kopaonik Mountains. There it receives numerous tributaries were coming from mountain slopes. The biggest of them are

rivers Drenska, Tvrdjanska, Jošanička, Leposavska, Sočanska, Bistrička, Vučanska, Banjska. During the rainy season, which usually occurs in April, May and sometimes in November, the water flow in the Ibar increases and represents a hazard for low-lying areas.

7.3.1 Neuro-Fuzzy Model for Water Flow Calculation

The series of climatic parameters were used as input parameters for the neuro-fuzzy modeling process. The first parameter was air temperature, the second parameter was vapor pressure, and the third parameter was humidity. In this study the reference evapotranspiration is analyzed based on several input parameters which represent weather parameters. There was a need for estimation which weather parameter has the highest influence for the reference evapotranspiration. The algorithm is based on evolutionary computation or genetic computation (Jovic et al. 2018a). After the estimation, the evapotranspiration was measured experimentally by weighing lysimeter. The soil weight was measured, and the change in water storage in the soil was modeled based on the weight change. Evapotranspiration was estimated as the weight changing with precipitation addition and percolation substitution. The percolation shows the movement and of fluids through porous materials. The used data was collected from WorldBank dataset for all countries in the European Union (Ilic et al. 2017).

In this study, the values of air temperature, vapor pressure, and humidity were used for generating the neuro-fuzzy model. Table 7.7 shows the statistical parameters of the input data. The neuro-fuzzy network was trained with the collected data from Table 7.7. Three bell-shaped membership functions were used for each input separately since the bell-shaped functions have the highest generalization capability. RMSE and R^2 were used as statistical indicators for the neuro-fuzzy prediction accuracy. Table 7.8 shows the statistical results for the neuro-fuzzy estimation for all vegetable months (April–September). It can be noted that the RMSE varies between 0.02 and 0.08 mm/day. The highest correlation coefficient could be observed for August. The lowest correlation coefficient could be noted for May. It is clear that the neuro-fuzzy model has good agreement with the experimental data for the vegetable period.

Table 7.7 Statistical parameters for neuro-fuzzy training process

Input parameters	Statistical parameters				
	Min.	Max.	Mean	Standard deviation	Variation coefficient
Air temperature (°C)	5.2	19.5	11.3	0.70	0.05
Vapor pressure (kPa)	0.6	1.3	1.00	0.06	0.04
Humidity (%)	44.8	88.7	77.96	2.13	0.06

Table 7.8 Performance statistics for the months in vegetable period

Indicator	Months					
	April	May	June	July	August	September
RMSE	0.08	0.07	0.02	0.05	0.07	0.06
R^2	0.91	0.92	0.95	0.95	0.98	0.94

7.3.2 Flood Risk Assessment

Flood hazards and flood prevention or mitigation measures can be different, depending on the flood characteristics. According to the Kosovo Flood Management Framework, there are three principal types of flooding relevant to Kosovo:

1. Large-scale lowland flooding
2. Flash flooding in upland areas
3. Flooding from a Dam failure

In Leposavić, Zvečan and Zubin Potok municipalities the floods can appear in three cases that are noted above (Stanojevic et al. 2018). The first case is the flood in Ibar valley, the second the case is when the floods can happen from the rivers of the Ibar branches of the river and the third case is if the floods can happen because of the damage of the Gazivode dam. The subject of this document is to value floods of the first case and the second case, since the third case is specific and the possibility to happen is very small. All branches of this river have torrential characteristics, which mean that the imbalance between the minimum and maximum quantity of water is big. These rivers are dangerous in the time when precipitations are big and last for a short time. Therefore, residents are not prepared, and the damages are significant, in humans, objects, and agricultural lands. The information on rivers and the catchments are enabled by the data presented through GIS, and presented in Table 7.9.

Based on the field data, the risk areas are categorized into three levels of risk. The infuleced areas are listed in the Table 7.10.

Even though all river Ibar tributaries has certain flooding capacity, as seen in the Table 7.10, the focus will be on the river Ibar area. The river Ibar is the main water body in the area, and the Gazivode lake was built to manage the river. The first risk area is situated near the dam, on the Lucka river, the tributary of Ibar. The floods are frequent because of the upper part of the river bed erosion and the material deposition in the lower part. The risk areas are graded as High (red), Medium (orange) and Low (yellow) risk areas as presented in the Fig. 7.8.

However, after the dam, the river Ibar goes out of the bed and floods the agriculture land and residential area.

1. First region—downstream from the discharge of Sitnica into Ibar (5 km)
2. Second region—downstream from the discharge of Ceranjska river (7.3 km).

Because of the abundant vegetation on its banks, and non degradable waste in the water, the river becomes overloaded, forming the bottlenecks contributing the floods

Table 7.9 River Ibar catchment properties

ID1	Perimeter	River_Name	AREA_m	AREA_km
1	55,264.18	Banjska r.	75,843,819.7	75.84
2	23,132.5	Jagnjenička r.	19,987,348.31	19.99
3	7485.39	Međeđi potok	3,048,587.65	3.05
4	11,036.62	Kuševski potok	5,148,055.1	5.15
5	30,705.83	Brosovačka r.	44,430,955.25	44.43
6	14,816.25	Zubin potok	8,595,347.04	8.60
7	4954.6	Bjelevode p.	871,906.01	0.87
8	6671.93	Radovića potok	1,749,144.35	1.75
9	7868.54	Čabranska	3,366,995.89	3.37
10	13,744.58	Zupčanska_reka	7,108,909.23	7.11
11	20,048.99	Dragočevska reka	15,551,783.12	15.55
12	7662.32	Vranovićki p.	2,930,181.2	2.93
13	7963.21	Banjski p.	2,728,652.18	2.73
14	20,154.91	Varaška reka	17,178,356.21	17.18
15	26,510.91	Brnjačka reka	33,143,367.15	33.14
16	24,791.79	Čečevska reka	24,619,430.65	24.62
17	12,957.26	Koriljska r.	7,874,550.13	7.87
18	33,652.05	Koriljska r.	26,800,200.24	26.80
19	18,325.67	Seoska r.	13,379,825.81	13.38
20	38,751.45	Vučanska r.	28,809,803.21	28.81
21	31,028.85	Grkajska r.	23,330,043.17	23.33
22	45,413.27	Josanička r.	57,133,153.57	57.13
23	20,030.79	Borova r.	18,746,170.04	18.75
24	30,645.81	Vračevska r.	38,610,419.68	38.61
25	17,022.18	Trebićka r.	11,181,421.85	11.18
26	9942.76	Trifunski p.	3,934,417.53	3.93
27	6339.9	Kremenjački p.	1,871,112.67	1.87
28	34,274.51	Dobravska r.	28,364,482.8	28.36
29	40,603.23	Sočanička r.	42,176,001.62	42.18
30	27,494.19	Ceranjska r.	22,113,452.14	22.11
31	10,291.9	Veliki p.	3,928,108.81	3.93
32	61,642.8	Bistrica	161,946,124.1	161.95
33	12,632.48	Doljenaška reka	7,020,047.33	7.02
34	11,171.77	Radevački p.	4,735,101.12	4.74
35	29,809.79	Leposavska r.	27,386,129.14	27.39
36	37,738.34	Tvrđanska r.	41,721,602.79	41.72

(continued)

Table 7.9 (continued)

ID1	Perimeter	River_Name	AREA_m	AREA_km
37	43,500.66	Drenska r.	61,804,284.54	61.80
38	13,136.88	Lešanska r.	6,868,945.76	6.87
39	10,536.51	Žigoljski p.	4,128,262.85	4.13
40	12,193.84	Ostrački p.	5,840,653.24	5.84
41	28,899.58	Bistrička Reka	31,401,376.29	31.40

(Fig. 7.9). In general, water flushes topsoil from the river banks, and even larger trees are falling to the river. It can be also a risk to the bridges, and it can lead to the fractures of the pillars. In the first region, the Ibar river is situated in the middle of two roads: Regional road Kosovska Mitrovica-Leposavić and railroad. These are the boundaries of the river, preventing the outflows over the roads. The Sitnica river is bringing large quantities of deposits and increases the river bed and consequently the water level. The industrial waste deposits are situated on the river Ibar banks— Gornje polje on the right bank, and Zarkov potok and Zitkovac on the left bank of the river, polluting the river with heavy metals and discharging the toxic solid materials through erosive canals and ditches into the river (Milentijevic et al. 2013). The second region is located downstream from the Ceranjska river discharge to the river Ibar. In this section, the following rivers are tributaries of the river Ibar: on the left side-Vučanska river and Grkajska river; on the right side: Ceranjska river, Zrinjski stream, Sočanička reka and Dobravska reka. Right side of the Ibar is limited by the regional road. The river profile is reduced as those tributaries bring the sediment and woods from the surrounding mountains. In the most of the cases, the agriculture land is impacted by the flood risk, as shown in the Fig. 7.10.

7.4 Conclusion

Based on the available data, it is clear that there are two periods of large waters during the year, and those happen in the spring and autumn, as well as one period of low waters in August. By analyzing the diagrams of monthly precipitations and characteristic flows (NQ, SQ, and VQ) in analyzed water meter stations, it is obvious that large waters mainly occur as a consequence of the heaviest precipitations. The maximum daily flow is proportional to heavy rain and snow melting.

In the observed area, runoff is very large, while, the infiltration of the precipitations into the ground waters is very low. According to some reports, only 15% of the precipitation is penetrating the unconfined bed and reaches the aquifer. It is concluded that the floods have happened as a result of erosion in the upper part of the river basin and alluvial sedimentation of these alluvial in the lower part of the river. Human activities have influenced this phenomenon (waste, trees, etc.) and also their inactivity (not maintenance of the river) has been the main factor that has contributed to flooding.

Table 7.10 Risk areas in the river Ibar catchment, and possible impacted infrastructure

ID1	River_Name	Category_Risk	Risk_Area	Infrastructure
65	Bistrička Reka	High	4331.49	Agricultural land
66	Vračevska Reka	High	2771.41	Agricultural land
67	Drenska Reka-3	High	7273.04	Agricultural land
68	Drenska Reka-2	High	4022.38	Agricultural land, wells
69	Drenska Reka-1	High	4313.84	Agricultural land
70	Tvrđanska Reka	High	23,599.6	Residential buildings, road, yards, agricultural land
71	Josanička Reka	High	6689.62	Agricultural land, road, substation
72	Sočanicka Reka	High	17,213.33	Agricultural land
73	Ibar-2	High	1,124,061.76	Agricultural land, bridges, roads
74	Vučanska Reka	High	25,769.83	Agricultural land, bridge, roads
75	Ceranjska Reka	High	3394.58	Agricultural land, roads
76	Banjska Reka	High	7999.69	School, residential building, road, yards, agricultural land
77	Lučka_Reka_2	High	4544.83	School, road, business building
78	Lucka_Reka_1	High	38,817.71	Agricultural land
79	Ibar-1	High	1,308,722.14	Agricultural land, bridges, roads
80	Kozarevska Reka	High	5861.6	Residential building, road, yards, agricultural land
81	Zubin Potok	High	25,287.4	Administration building, residential building, road, yards
82	Koriljska Reka	High	8582.1	Agricultural land
83	Jagnjenička Reka	High	1109.6	Agricultural land, bridge
84	Bistrička Reka	Low	6931.53	Agricultural land
85	Vračevska Reka	Low	17,327.76	Agricultural land, bridge
86	Drenska Reka-1	Low	6617.68	Agricultural land
87	Tvrđanska Reka	Low	45,966.24	Residential buildings, road, yards, agricultural land
88	Jošanička Reka	Low	10,332.38	Agricultural land, road, substation
89	Sočanička Reka	Low	30,141.93	Agricultural land

Table 7.10 (continued)

ID1	River_Name	Category_Risk	Risk_Area	Infrastructure
95	Vučanska Reka	Low	38,053.5	Agricultural land, bridge, roads, residential building, fish pond
96	Ceranjska Reka	Low	14,918.47	Agricultural land, roads
98	Banjska Reka	Low	13,212.38	School, residential building, road, yards, agricultural land
99	Lučka_Reka_2	Low	7558.21	School, road, business building
100	Lučka_Reka_1	Low	63,332.76	Agricultural land
101	Kozarevačka Reka	Low	8027.91	Residential building, road, yards, agricultural land
102	Ibar-1	Low	1,540,323.64	Agricultural land, bridges, roads
103	Zubin Potok	Low	32,749.99	Administration building, residential building, road, jards
104	Koriljska Reka	Low	15,125.7	Agricultural land
105	Jagnjenička Reka	Low	3467.02	Agricultural land, bridge
110	Ibar-2	Low	1,512,430.58	Agricultural land, bridges, roads
111	Lučka_Reka_1	Medium	3338.71	Agricultural land
112	Lučka_Reka_1	Medium	7280.11	Agricultural land
113	Lučka_Reka_2	Medium	433.58	School, road, business building
114	Jagnjenička Reka	Medium	137	Agricultural land
115	Koriljska Reka	Medium	2338.37	Agricultural land
116	Ibar-1	Medium	16,555.6	Agricultural land
117	Ibar-1	Medium	7656.11	Agricultural land
118	Josanička Reka	Medium	304.86	Agricultural land
119	Josanička Reka	Medium	223.23	Agricultural land
120	Josanička Reka	Medium	126.06	Agricultural land
121	Ibar-2	Medium	27,562.13	Agricultural land
122	Ceranjska Reka	Medium	406.99	Agricultural land, roads
123	Tvrđanska Reka	Medium	1909.01	Agricultural land

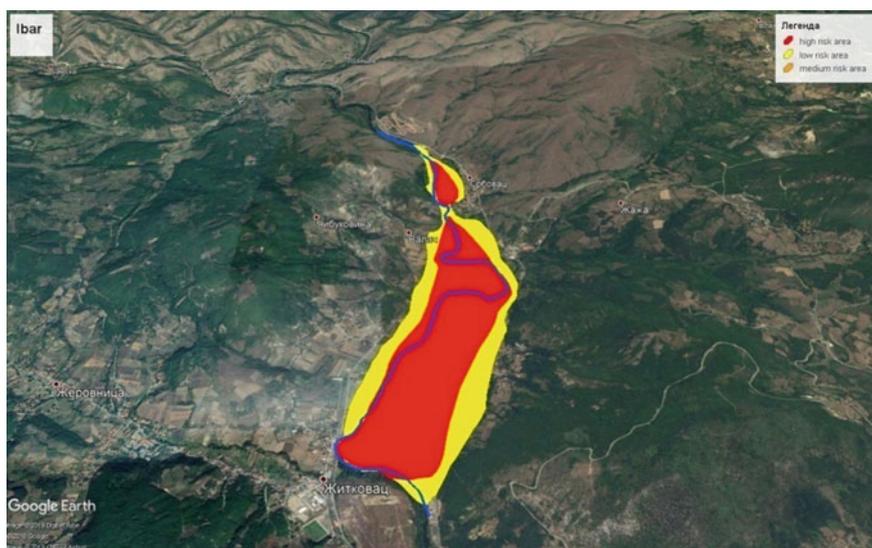**Fig. 7.8** Flood risk assessment of the Lucka river (Color Figure Online)

Fig. 7.9 Endangered regions in the river Ibar area downstream from the river Sitnica discharge (Color figure online)
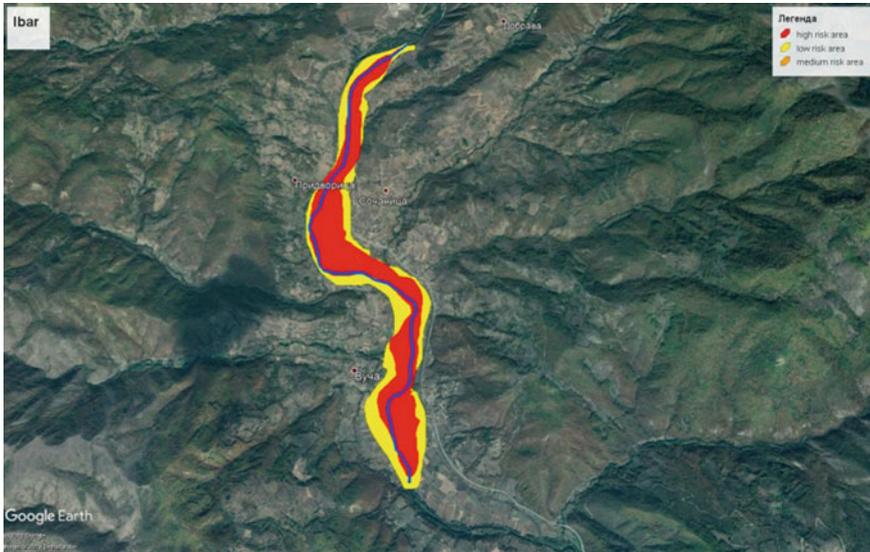
Fig. 7.10 Endangered areas downstream from the discharge of Ceranjska river and Sitnica (Color figure online)

References

Blum, U., & Gerig, T. M. (2006). Interrelationships between p-coumaric acid, evapotranspiration, soil water content, and leaf expansion. *Journal of Chemical Ecology, 32*(8), 1817–1834.

Buchtele, J., & Tesar, M. (2009). The time variability of evapotranspiration and soil water storage in long series of rainfall-runoff process. *Biologia, 64*(3), 575–579.

Cai, C. Z., Zhu, X. J., Wen, Y. F., Pei, J. F., Wang, G. L., & Zhuang, W. P. (2010). Predicting the superconducting transition temperature T c of BiPbSrCaCuOF superconductors by using support vector regression. *Journal of Superconductivity and Novel Magnetism, 23*(5), 737–740.

de la Paix Mupenzi, J., Li, L., Ge, J., Ngamije, J., Achal, V., Habiyaremye, G., et al. (2012). Water losses in arid and semi-arid zone: Evaporation, evapotranspiration and seepage. *Journal of Mountain Science, 9*(2), 256–261.

Djokic, J., Minic, D., Kamberovic, Z., & Petkovic, D. (2012). Impact analysis of airborn pollution due to magnesium slag deposit and climatic changes condition. *Ecological Chemistry and Engineering, 19*(3), 439–444.

Dong, Q., Zhan, C., Wang, H., Wang, F., & Zhu, M. (2016). A review on evapotranspiration data assimilation based on hydrological models. *Journal of Geographical Sciences, 26*(2), 230–242.

Gao, G., Xu, C. Y., Chen, D., & Singh, V. P. (2012). Spatial and temporal characteristics of actual evapotranspiration over Haihe River basin in China. *Stochastic Environmental Research and Risk Assessment, 26*(5), 655–669.

Gerla, P. J. (1992). The relationship of water-table changes to the capillary fringe, evapotranspiration, and precipitation in intermittent wetlands. *Wetlands, 12*(2), 91–98.

Gocic, M., Shamshirband, S., Razak, Z., Petković, D., Ch, S., & Trajkovic, S. (2016). Long-term precipitation analysis and estimation of precipitation concentration index using three support vector machine methods. *Advances in Meteorology*, (Article ID 7912357), 11. https://doi.org/10.1155/2016/7912357.

Gong, Y., Zhang, Y., Lan, S., & Wang, H. (2016). A comparative study of artificial neural networks, support vector machines and adaptive neuro fuzzy inference system for forecasting groundwater levels near lake Okeechobee, Florida. *Water Resources Management, 30*(1), 375–391.

Ilic, M., Jovic, S., Spalevic, P., & Vujicic, I. (2017). Water cycle estimation by neuro-fuzzy approach. *Computers and Electronics in Agriculture, 135,* 1–3.

Itier, B., Flura, D., Belabbes, K., Kosuth, P., Rana, G., & Figueiredo, L. (1992). Relations between relative evapotranspiration and predawn leaf water potential in soybean grown in several locations. *Irrigation Science, 13*(3), 109–114.

Jang, J. S. R., Sun, C. T., Mizutani, E. (1997). *Neuro-fuzzy and soft computing: A computational approach to learning and machine intelligence*.

Jovic, S., Nedeljkovic, B., Golubovic, Z., & Kostic, N. (2018a). Evolutionary algorithm for reference evapotranspiration analysis. *Computers and Electronics in Agriculture, 150,* 1–4.

Jovic, S., Vasic, P., & Jaksic, T. (2018b). Sensorless estimation of lake level by soft computing approach. *Sensor Review, 38*(1), 117–119.

Kakahaji, H., Banadaki, H. D., Kakahaji, A., & Kakahaji, A. (2013). Prediction of Urmia lake water-level fluctuations by using analytical, linear statistic and intelligent methods. *Water Resources Management, 27*(13), 4469–4492.

Kalaba, D. V., Ivanović, I., Čikara, D., & Milentijević, G. (2014). The Initial analysis of the River Ibar temperature downstream of the lake Gazivode. *Thermal Science, 18*(1), 73–80.

Kisi, O., & Yildirim, G. (2005). Discussion of "Forecasting of reference evapotranspiration by artificial neural networks" by Slavisa Trajkovic, Branimir Todorovic, and Miomir Stankovic. *Journal of Irrigation and Drainage Engineering, 131*(4), 390. https://doi.org/10.1061/(ASCE)0733-9437(2005)131:4(390).

Liu, Y., Zhuang, Q., Pan, Z., Miralles, D., Tchebakova, N., Kicklighter, D., et al. (2014). Response of evapotranspiration and water availability to the changing climate in Northern Eurasia. *Climate Change, 126*(3–4), 413–427.

Meng, J., & Xia, L. (2007). Support vector regression model for millimeter wave transitions. *International Journal of Infrared and Millimeter Waves, 28*(5), 413–421.

Milentijević, G., Spalević, Ž., Bjelajac, Ž., Djokić, J., & Nedeljković, B. (2013). Impact analysis of mining company 'Trepča' to the Contamination of the river Ibar Water, National Vs. European law regulations. *Metalurgia International, 18,* 283–288.

Morari, F., & Giardini, L. (2001). Estimating evapotranspiration in the Padova botanical garden. *Irrigation Science, 20*(3), 127–137.

Qin, D., Lu, C., Liu, J., Wang, H., Wang, J., Li, H., et al. (2014). Theoretical framework of dualistic nature–social water cycle. *Chinese Science Bulletin, 59*(8), 810–820.

Rana, G., Katerji, N., Mastrorilli, M., & El Moujabber, M. (1997). A model for predicting actual evapotranspiration under soil water stress in a Mediterranean region. *Theoretical and Applied Climatology, 56*(1–2), 45–55.

Sanikhani, H., Kisi, O., Kiafar, H., & Ghavidel, S. Z. Z. (2015). Comparison of different data-driven approaches for modeling lake level fluctuations: the case of Manyas and Tuz lakes (Turkey). *Water Resources Management, 29*(5), 1557–1574.

Shafaei, M., & Kisi, O. (2016). Lake level forecasting using wavelet-SVR, wavelet-ANFIS and wavelet-ARMA conjunction models. *Water Resources Management, 30*(1), 79–97.

Stanojevic, P., Djokic, J., Zivkovic, B., & Rajovic, J. (2018). GIS application in floods risk assessment in Leposavic. In Proceedings of *9th GRACM International Congress on Computational Mechanics*, Chania, June 4–6, 2017 (pp. 195–201).

Tongal, H., & Berndtsson, R. (2014). Phase-space reconstruction and self-exciting threshold modeling approach to forecast lake water levels. *Stochastic Environmental Research and Risk Assessment, 28*(4), 955–971.

Trajkovic, S., & Kolakovic, S. (2010). Comparison of simplified pan-based equations for estimating reference evapotranspiration. *Journal of Irrigation and Drainage Engineering, 136*(2), 137–140.

Vaheddoost, B., Aksoy, H., & Abghari, H. (2016). Prediction of water level using monthly lagged data in lake Urmia, Iran. *Water Resources Management, 30*(13), 4951–4967.

Verplancke, T., Vanlooy, S., Benoit, D., Vansteelandt, S., Depuydt, P., Deturck, F., et al. (2008). Prediction of hospital mortality by support vector machine versus logistic regression in patients with a haematological malignancy admitted to the ICU. *Critical Care, 12*(2), 1.

Weng, X. Y., Xu, H. X., Yang, Y., & Peng, H. H. (2008). Water-water cycle involved in dissipation of excess photon energy in phosphorus deficient rice leaves. *Biologia Plantarum, 52*(2), 307–313.

World Bank Document: Water Security for Central Kosovo NO. 71850. (2011). The Kosovo-Iber River Basin and Iber Lepenc Water System.

Xu, J., Lv, Y., Ai, L., Yang, S., He, Y., & Dalson, T. (2016). Validation of dual-crop coefficient method for calculation of rice evapotranspiration under drying—Wetting cycle condition. *Paddy and Water Environment*, 1–13.

Xu, M., Ye, B., Zhao, Q., Zhang, S., & Wang, J. (2013). Estimation of water balance in the source region of the Yellow River based on GRACE satellite data. *Journal of Arid Land, 5*(3), 384–395.

Zhao, L., Xia, J., Xu, C. Y., Wang, Z., Sobkowiak, L., & Long, C. (2013). Evapotranspiration estimation methods in hydrological models. *Journal of Geographical Sciences, 23*(2), 359–369.